

**Robotic in-situ and satellite based observations of pigment and particle distributions in the Western North Atlantic**

E. Boss, D. Swift, L. Taylor, P. Brickley, R. Zaneveld, S. Riser, M.J. Perry

Emmanuel Boss<sup>1</sup>, Lisa Taylor, and Peter Brickley

School of Marine Sciences, University of Maine, Orono, Maine 04469

Dana Swift and Steve Riser

School of Oceanography, University of Washington, Seattle, Washington 98195-7940

J. Ronald V. Zaneveld

WET Labs, Inc., P.O. Box 518, 620 Applegate Street, Philomath, Oregon 97370

Mary Jane Perry

Ira C. Darling Marine Center and School of Marine Sciences, University of Maine, Walpole,  
Maine 04573

---

<sup>1</sup> Corresponding author (emmanuel.boss@maine.edu).

## **Acknowledgments**

This work has been made possible with funding from the Ocean Biology and Biogeochemistry Program of the National Aeronautics and Space Administration (NASA) under grant number NAG5-12473. Thanks to Dr. Peter Strutton for providing help in the float deployment.

Discussions with Drs. F. Chai and M. Behrenfeld are gratefully acknowledged.

## **Abstract**

Profiling floats equipped with optical sensors can extend satellite ocean color data to depth as well as provide data during periods and areas that suffer from cloud cover. Here we demonstrate this ability with a profiling float that obtained continuous high quality optical data for a period of three years without noticeable sensor drift. Good agreement was found with corresponding satellite ocean color. In addition the relationship between chlorophyll and particulate backscattering derived from the float measurements are found to be consistent with previously published data.

Upper ocean biogeochemical dynamics are evidenced in the float measurements displaying strong seasonal patterns associated with phytoplankton blooms as well as increase in pigmentation per particle at low light. However, unlike observations at low latitudes, surface optical variables are found to have shorter de-correlation scales than physical variables suggesting that biogeochemical processes control much of the variability observed.

The float spent 2.25yrs in the Sub-polar North Atlantic between Newfoundland and Greenland before crossing the North Atlantic Current (NAC) to warmer waters. An unusual eddy was sampled following the crossing of the NAC for a period of three months period. This anti-cyclonic feature contained elevated particulate material from surface to 1000db depth, the only such event in the floats' record. The eddy was associated with a weakly elevated pigment and backscattering at the surface but its depth integrated backscattering is similar to that during spring blooms. Such eddies, if frequent, are likely to have a large impact on particle delivery to depth, but have seldom been observed.

## Introduction

Upper ocean processes have long been known to regulate phytoplankton vertical distribution, bloom dynamics and primary production (e.g. Riley et al. 1949; Sverdrup 1953; Smetacek and Passow 1990; Denman and Gargett 1983), through their influence on nutrients and light availability to phytoplankton. Unfortunately, measuring primary production (NPP) directly and routinely over the appropriate temporal and spatial scales relevant to study the ocean's role in global elemental cycling and climate is not practical from shipboard observations and therefore efforts have been directed to estimate primary production from remotely observed ocean color.

At this time, however, remotely sensed ocean color cannot alone provide highly accurate phytoplankton standing stocks and NPP estimates in the upper ocean since: 1. no consensus exists regarding the appropriate algorithms to obtain NPP and their uncertainties, 2. ocean color provides only surface observations requiring assumptions to estimate the subsurface distribution, 3. ocean color chronically under samples cloudy regions, and 4. the atmosphere provides nearly 95% of the signal retrieved by the satellite requiring a significant effort be dedicated to the atmospheric correction of the signal. Since any bias in estimated NPP and algal standing stocks directly affect oceanic carbon budgets, reducing uncertainties in ocean color based algorithms will directly contribute to a better accounting of the role of the oceans in the carbon cycle and to study the climate driven changes in the Earth's biosphere.

Here we demonstrate the use of robotic in-situ observations of optical properties needed to study phytoplankton, primary production and particulate organic carbon recorded by an autonomous profiling float to assist in validation of ocean color remote sensing. In addition to measuring relevant algal and particulate carbon parameters throughout the year, the float

provides measurements in cloudy conditions and as a function of depth, generating needed information to further constrain relevant parameters for the calculation of NPP. The float also provides the distribution of biogeochemical parameters as a function of depth. Together with physical data (both collected by the float and remotely observed) the link between upper ocean dynamics and its biogeochemistry can be studied.

Profiling floats measuring physical parameters such as temperature and salinity have been in operation since the late 1990s and are part of an international observation network (ARGO, e.g. Gould et al. 2004). However, very few profiling floats have been fitted with sensors that monitor the ocean's biogeochemistry. Recent effort has been undertaken to push for the addition of oxygen sensors to the ARGO floats (Kortzinger et al. 2006). The float described in this paper was equipped with optical sensors capable of providing estimates for the standing stock of particles and phytoplankton chlorophyll *a* pigment.

Optical properties such as the diffuse attenuation coefficient and beam attenuation have been previously measured with profiling floats (Mitchell et al. 2000; Bishop et al. 2002 & 2004) during season-long targeted experiments investigating the dynamics of phytoplankton and particulate organic materials in the upper ocean. Here we showcase the use of profiling floats for long-term (three years) and routine observations of hydrographical and optical properties in the upper ocean.

## Material and methods

A Webb Research Corp. APEX float was fitted with a Sea-Bird Electronics SBE41 CTD, a custom flat-faced WET Labs hockey-puck size optical sensor that measures side scattering at 880nm (analogous to WET Labs' LSS, e.g. Baker et al. 2001), and a chlorophyll *a* fluorometer (470nm excitation, 680nm emission, analogous to the commercially available WET Labs' ECO fluorometer). An oxygen sensor was also deployed on the float but failed within the first six months of launch; hence, data are not reported. Sensors were integrated into the float using a Webb Research Corp. Apf9a controller. The float and sensors were tested for pressure endurance in a pressure tank simulating 50 dive cycles to 1200db recording data throughout the test to evaluate possible effects of pressure on sensor performance.

The float was deployed at 51.84N 48.43W on 12 June 2004 (Fig. 1). The mission was designed such that the float collected data on its upward trajectory from 1000db to the surface every five days, collecting data at approximately 50 depths during each profile with closer spacing between sampling depths close to the surface and sparser spacing at depth. The float surfaced close to midnight (local time at the location of its launch) to ensure that chlorophyll *a* fluorescence measurements were not biased by non-photochemical quenching (e.g. Luftus and Seliger, 1975); as the sun rose, we often observed reductions in fluorescence. A similar effect has often been observed with fluorometers deployed on other autonomous vehicles such as gliders (Sackmann, 2007). The float subsequently spent approximately 10h. at the surface, sending data to the ARGOS satellite and continuing to collect optical surface data before returning to its parking depth at 1000db.

The optical sensors used provide an output that is linearly related to side scattering at 880nm and fluorescence excited at 470nm and emitted at 680nm. The linear relationship between

signal measured and scattering or fluorescence is comprised of a constant (the signal measured in the absence of material scattering or fluorescence, the dark signal) and a slope which relates the measured signal minus the dark signal to the concentration of the material. The dark signal was established (following the manufacturer's recommendation) by covering the detector with black tape and immersing the instrument in water while recording the output signal. Coefficients to convert digital counts to backscattering units at 440nm ( $m^{-1}$ ) and chlorophyll units ( $mg\ m^{-3}$ ) were determined with a vicarious calibration procedure using a type-II regression analysis of APEX float optical data and interpolated chlorophyll and particulate backscattering coefficient data obtained from an inversion of satellite ocean color (see below). We used nighttime fluorescence data from the surface and median values for scattering from the upper 5-15db depths to avoid contamination by bubbles (observed as spikes on some occasions).

Ocean color remote sensing products were obtained from <http://oceancolor.gsfc.nasa.gov/PRODUCTS/>. Here we used NASA's standard chlorophyll product for Moderate Resolution Imaging Spectroradiometer (MODIS) and computed the particulate backscattering coefficient at 440nm ( $b_{bp}(440)$ ) by performing an inversion on the normalized water leaving radiances with the algorithm outlined in Maritorena et al. (2002). Level 2 data were processed as follows: all satellite passes within a six-hour period, which amount to all data collected within a daylight period, were averaged into a single scene. Subsequently the data were median-averaged over the non-masked data pixel found within 7.5km of the float's most recent location. For the vicarious calibration described above, the ocean-color data were interpolated to the time of the float surfacing ( $n=202$  for  $b_{bp}$  and  $n=208$  for chlorophyll). The 7.5km scale was based on a spatial decorrelation analysis (not shown) and agrees with the local baroclinic radius of deformation (e.g. Smith et al. 2000). We tested for contamination of pixels

adjacent to clouds by applying a dilation operator; cloud masked regions are enlarged by a binary dilation operation with a disk shaped kernel (two pixel radius) to remove cloud edge effects (Gonzales and Woods, 1992). This operation reduced the number of available remotely sensed spectra obtained for 12 June 2004 to 1 May 2007 from 233 to 150 without changing significantly either the correlation coefficient or the calibration slope between in-situ data and those inverted from satellite. We thus elected not to use the dilation procedure.

The scattering sensor on the float measured side scattering at 880nm. The sensor was designed to be a turbidity sensor and thus its calibration was to Nephelometric Turbidity Units (NTU) which is not easily translatable to physical units used in optics. Our own observations and those of M. Twardowski (pers. communication) show that side scattering (measured with WETLabs' LSS) is very well correlated to backscattering measurements in most oceanic environments where the particle size distribution is relatively constant. Side scattering was vicariously calibrated to backscattering units at 440nm [ $\text{m}^{-1}$ ] using remotely sensed ocean color as described above. While one could expect uncertainties in such vicarious calibration to be +/- 100%, data presented below suggest that the uncertainties in  $b_{bp}(440)$  are significantly smaller. In any case, no data presented here depend on a high level of accuracy in the estimate of  $b_{bp}(440)$ . From here on we will refer to the float's scattering measurement as  $b_{bp}(440)$ .

Nighttime chlorophyll fluorescence was vicariously calibrated to chlorophyll concentration [ $\text{mg m}^{-3}$ ] using the standard NASA product. Although chlorophyll fluorescence has been used in situ as a proxy for chlorophyll *a* concentration since the 1960's (Lorenzen, 1966), the plasticity in the fluorescence quantum yield due to non-photochemical quenching, chlorophyll packaging, variation in relative accessory pigment concentrations, nutrient limitation, etc. makes absolute calibration of fluorescence challenging. Nevertheless, given the



large dynamic range in the signals observed by the float, chlorophyll fluorescence provides a useful and unique proxy of phytoplankton biomass. We did not use the manufacturer calibration slope coefficient for chlorophyll as it is based on a laboratory phytoplankton culture that may not be relevant to the species and local growth conditions in the water sampled by the float. NASA advertises its chlorophyll product to be on average within 30% of true value. Given uncertainties both in the conversion of fluorescence to chlorophyll and ocean color to chlorophyll, the conversion coefficient for chlorophyll concentration is likely to have larger uncertainty than for backscattering. However, no data presented here depend on a high level of accuracy in the estimated chlorophyll concentration.

Scattering has been found to be a good proxy for particulate volume, mass and particulate organic carbon (Spinrad and Zaneveld 1982; Babin et al. 2003). Recent work suggests that the phytoplankton contribution to the total particulate material in the upper ocean is often constrained between 25 and 40% across seasons at one location (DuRand et al. 2001) and across different trophic regions (Oubelkheir et al. 2005). As a check for our calibration procedure, we estimate the phytoplankton carbon concentration from backscattering measurements near the surface using the equation (Behrenfeld et al. 2005):  $C_{\text{phytoplankton}} = 13000 \times (b_{\text{bp}}(440) - 0.00035)$ . Together with the chlorophyll (Chl) measurements, we obtain a  $C_{\text{phytoplankton}}/\text{Chl}$  ratio with a median value of 63g C/g Chl (5<sup>th</sup> percentile=26g/g, 95<sup>th</sup> percentile=183g/g), consistent with field and laboratory values for nutrient-sufficient phytoplankton growing at high irradiances (e.g. Cloern et al., 1995).

Sea surface height anomaly data with  $\frac{1}{4}^\circ$  degree resolution were obtained from the Colorado Center for Astrodynamics Research at the University of Colorado, Boulder. Data were processed as in Leben et al. (2002).

## Results

### *Sensor stability and validation*

Float 0005 accomplished 221 profiles of the upper 1000m of the Western North Atlantic Ocean, once every five days since its launch in June 2004 through 22 June 2007. The float spent most of its mission in the Subpolar Gyre before crossing the North Atlantic Current (NAC) in September 2006 into the warmer waters to its south (Fig. 1). After crossing the NAC, the float spent approximately 3 months within an anti-cyclonic eddy with highly elevated backscattering values (see below).

Data from 950m and below suggest the float sensors were stable over the three-year mission (Fig. 2). Except for rare spikes in the back-scattering coefficient, and the higher values associated with passage through an eddy, the deep values are approximately constant ( $\sim 0.0015\text{m}^{-1}$ ). Surface data also correlate well with similar variables obtained from satellite ocean color, further supporting the hypothesis that the sensors did not drift during the three-year mission (Fig. 3.) Although the same data were used to derive the coefficients to convert digital to calibrated data, the consistent correlation ( $R=0.88$  for chlorophyll and  $0.90$  for backscattering) over three years supports our hypothesis of little drift in the optical sensors.

The relationship between particulate backscattering and chlorophyll are also consistent with relationships derived from in-situ measurements in the Southern Ocean by Reynolds et al. (2001) and with relationships derived from ocean color (Behrenfeld et al., 2005), but are not consistent with that of Wang et al. (2005) based on in-situ data collected in the Arctic Ocean (Fig. 4).

### *Upper ocean dynamics*

Phytoplankton surface distributions are spatially patchy ( $O(1)$  deformation radius here  $\sim 10\text{km}$ ) and have the potential to be highly variable temporally due to growth rates (being on the order of a day), grazing and meso-scale dynamics. Thus one may expect data to be highly uncorrelated between subsequent profiles. Here we find the near-surface optical properties (and thus biogeochemistry) to have shorter de-correlation time scales than the physical properties, with chlorophyll having the shortest de-correlation time scale with e-folding time of nearly two weeks (Fig. 5).

The float spent a little more than two years in the Subpolar Western North Atlantic (Fig. 1). The annual cycle dominates the variability with warming between February and late August and subsequent cooling (Figs. 3, 6). The near-surface chlorophyll and backscattering coefficients in the upper ocean are always higher than at depth and exhibit a rapid rise in the spring and a slower decrease in the fall and winter. The chlorophyll and backscattering coefficients are well correlated ( $R > 0.86$ ) in the upper 300m consistent with backscattering being dominated by phytoplankton and particles that covary with phytoplankton (Fig. 4). Note, however, that below the mixed layer, a significant increase in chlorophyll/ $b_{bp}$  ratio is observed in the summer, consistent with photo-acclimation of cells to low light (Fig. 6). This ratio increases for the same reason near the surface in the winter. At greater depths no significant signal in pigments is observed while the seasonal modulation in backscattering is observed all the way to the deepest depth bin (750-1050db) though with an amplitude that is two orders of magnitude smaller than at the surface and a maximum which is shifted later in the year relative to the surface's particle concentration maximum (Fig. 7).

### *Effects of clouds*

To assess the usefulness of the float's ability to sample under clouds we compared the temporal coverage available by the float to that of the satellite (Fig. 8). While in summer months we obtained better coverage from remote sensing, during the winter the float coverage was superior within the 7.5km radius around the float's latest position.

To determine whether superior coverage by the float in the winter could translate to better monthly mean data, we computed the ratio of the monthly standard deviation to the monthly mean (the coefficient of variation, Fig. 8). During cloudy periods (when the number of satellite samples is low) the coefficient of variation in optical properties is usually low. Sunny periods, associated with many ocean color observations, are also associated with a large coefficient of variation. This variance, however, is often captured by the more frequent satellite ocean color measurements.

### *The eddy event*

An unusual eddy was sampled by the float in the fall of 2006 following the crossing of the Gulf Stream; this eddy was quasi-stationary from September to mid-November (not shown), had a small expression in surface ocean color data (relative to measurements before and after its encounter, Fig. 3) and was observed well in altimetry data (Fig. 9). While encircling the eddy the float recorded the only occasion of significant elevated scattering above background at depths below 950db (Fig. 2). Depth-integrated chlorophyll values show little signal associated with the eddy, however integrated  $b_{bp}$  values show a signal which is comparable in magnitude to that observed during the spring bloom (Fig. 10).

## **Discussion and conclusions**

We have demonstrated the ability to measure optical variables for a period of three years on a profiling float. The data quality was maintained with no fouling observed. This is possibly attributable to the mission profile which includes a large fraction of time in the deep dark and cold ocean and a relatively short stay at the surface (about ten hours every five days and mostly at night).

Agreement with remotely sensed observations showcase the potential to use similar sampling platforms for validation of satellite remote sensing. In addition, as demonstrated here, it allows for testing of potential biases in monthly mean values due to cloud conditions. Here we find that within the Sub-polar Gyre the periods of low satellite coverage (i.e., winter) are correlated with low variability in chlorophyll suggesting that in that at high latitudes in winter clouds do not significantly bias remotely estimated monthly means. This correlation is because winter is associated with low temperature and lower averaged mixed layer light-levels, both of which are likely to decrease phytoplankton growth rates.

Agreement of our backscattering coefficient to chlorophyll relationship with published ones suggests that the vicarious calibration approach we have used here works. It is, however, advisable to use physically calibrated backscattering sensors (rather than turbidity sensors calibrated to NTUs) as well as to calibrate chlorophyll fluorometers with extracted chlorophyll from local phytoplankton populations.

Autocorrelation analysis of the whole data set reveals chlorophyll to have a shorter decorrelation time scale than backscattering. This is likely due to the ability of phytoplankton to rapidly (within a generation time scale) alter their intercellular chlorophyll concentration in

response to changes in light and nutrients. It may also suggest that backscattering is not responding only to material that covaries with phytoplankton.

The de-correlation time scales observed by the float are significantly longer than the O(2days) de-correlation time scales calculated by Strutton and Chavez (2003) for chlorophyll obtained from ocean color data from the equatorial Pacific and the O(4days) de-correlation time scale calculated for in-situ chlorophyll from drifters in the California current by Abbott and Letelier (1998). This may seem surprising given the shorter deformation radius in the North Atlantic. The reason for the longer de-correlation time scale observed with the float is the significantly larger seasonal signal in the North Atlantic, which dominates the observed variability as well as possibly the reduced growth rates by phytoplankton in the cold water of the Western North Atlantic (Eppley, 1972). Denman and Abbott (1994) and Abbott and Letelier (1998) observed equal de-correlation time scales for temperature and chlorophyll while here we observe shorter de-correlation time scales for all the optical variables compared to the hydrographic variables. Strutton and Chavez (2003) interpret covariation in de-correlation time scales as being a sign of causality. Under that interpretation, our observation suggests that phytoplankton in the Western North Atlantic is significantly modulated by other processes than those responsible for variability in the upper ocean's hydrography.

A particle rich eddy was sampled in the late fall of 2006 which had little surface expression in ocean color. Its particle load is observed coherently through the 1000db water column suggesting it may be responsible for a large flux of particles to depth. This event is reminiscent of observations at the Bermuda Atlantic Time Series (BATS, Conte et al. 2003) where during some winters large flux of biogenic materials were collected in 3000db sediment traps associated with an eddy feature but with little surface expression in chlorophyll. Currently

we do not have a mechanism to explain the processes that formed or concentrated the material within the eddy; settling velocities of micron size particle cannot explain the temporal coherence between near surface measurements and those at 1000db. Additionally, no anomalous atmospheric transmission values, possibly associated with a dust deposition event, occurred during that time.

Eddies such as that sampled by the float and those observed at BATS could be very important (even dominant) in the global biogeochemical inventory of carbon and its flux to depth. However, currently we cannot account for such contributions due to our inability to sample the subsurface ocean from space and the limited space and time scales observed using ship board observations or single point moorings which cannot capture many realizations of such eddies.

It is our hope that the success and results demonstrated here will encourage the addition of biogeochemical sensors to the existing and planned fleet of robotic platforms in the world's ocean. Such a fleet will provide necessary inputs and constraints for ocean scale biogeochemical and ecosystem models which are necessary to increase our understanding of the role the oceans are playing in biogeochemical cycling in general and in recent climate processes in particular.

If a fleet of biogeochemical profiling floats were to operate throughout the world's ocean, the contribution of the mesoscale band to important biogeochemical fluxes could be constrained. Such a fleet exists for the measurements of hydrographical properties. A coordinated effort by the oceanographic community, such as the current effort to include oxygen measurements as part of the ARGO program, could make it a reality.

In addition, ecosystem and biogeochemical ocean models are starting to use optical variables to better model the underwater light field (e.g. for photosynthesis and photo-oxidation)

and constrain biogeochemical variables (e.g. Fujii et al., 2007). Data such as that collected by the float discussed here could provide these models with much needed ground truth resulting in increased skill.

Newer communication technologies such as satellite cell phones (e.g. iridium) can significantly improve future float missions; since they allow for significantly shorter stays at the surface (to less than an hour per profile), two-way communication (allowing for adaptive sampling), and provide for higher vertical resolution of data for the same amount of power.



## References

- Abbott, M. R. and R. M. Letelier. 1998. Decorrelation scales of chlorophyll as observed from bio-optical drifters in the California Current. *Deep-Sea Res. II*, 45, 1639-1667.
- Babin, M., A. Morel, V. Fournier-Sicre, F. Fell, and D. Stramski. 2003. Light scattering properties of marine particles in coastal and open ocean waters as related to the particle mass concentration. *Limnol. Oceanogr.* **48**: 843–859.
- Baker, E. D., A. Tenant, R. A. Feely, G. T. Lebon, and S. L. Waker. 2001. Field and laboratory studies on the effect of particle size and composition on optical backscattering measurements in hydrothermal plumes. *Deep-Sea Res. I* **48**: 593–604.
- Behrenfeld, M.J., E. Boss, D.A. Siegel, and D.M. Shea. 2005. Carbon-based ocean productivity and phytoplankton physiology from space. *Global Biogeochem. Cycles* **19**: GB1006, doi:10.1029/2004GB002299.
- Bishop, J.K.B., R.E. Davis, and J.T. Sherman. 2002. Robotic observations of dust storm enhancement of carbon biomass in the North Pacific. *Science* **298**: 817-821.
- Bishop, J.K.B., T.J. Wood, R.E. Davis, and J.T. Sherman. 2004. Robotic observations of enhanced carbon biomass and export at 55S. *Science* **304**: 417-420.
- Cloern, J. E., C. Genz, and L. Vidergar-Lucas. 1995. An empirical model of phytoplankton chlorophyll: carbon ratio - the conversion factor between productivity and growth rate. *Limnol. Oceanogr.* **40**: 1313–1321.

- Conte, M.H., T.D. Dickey, J.C. Weber, R. Johnson, and A. Knap. 2003. Transient physical forcing of pulsed export of bioreactive material to the deep Sargasso Sea. *Deep-Sea Res. I* **50**: 1157-1187.
- Denman, K. L., and A. E. Gargett. 1983. Time and space scales of vertical mixing and advection of phytoplankton in the upper ocean. *Limnol. Oceanogr.* **28**: 801-815.
- Denman, K. L. and M. R. Abbott. 1994. Time scales of pattern evolution from cross-spectrum analysis of advanced very high resolution radiometer and coastal zone color scanner. *J. Geophys. Res.* **99**: 7433-7442.
- DuRand, M. D., R. J. Olson, and S. W. Chisholm. 2001. Phytoplankton population dynamics at the Bermuda Atlantic time-series station in the Sargasso Sea. *Deep-Sea Res. II* **48**: 1983– 2003.
- Eppley, R. W. 1972. Temperature and phytoplankton growth in the sea. *Fish. Bull.* **70**: 1063-1085.
- Gould, J., et al. 2004. Argo profiling floats bring new era of in situ ocean observations. *Eos Trans. AGU* **85(19)**: 185.
- M. Fujii, E. Boss, and F. Chai. 2007. The value of adding optics to ecosystem models: a case study. *Biogeosciences Discuss.*, 4, 1585-1631, 2007 SRef-ID: 1810-6285/bgd/2007-4-1585
- Körtzinger, A., S. C. Riser, and N. Gruber. 2006. Oceanic oxygen: the oceanographer's canary bird of climate change. *Argo Newsletter Argonautics* 7 **June 2006**: 2-3.
- Leben, R. R., G. H. Born, B. R. Engebret. 2002. Operational altimeter data processing for mesoscale monitoring. *Marine Geodesy* 25: 3-18.

- Lorenzen, C. J. 1966. A method for the continuous measurement of in vivo chlorophyll concentration. *Deep-Sea Res.* **13**: 223-227.
- M. E. Loftus and H. H. Seliger. 1975. Some limitations of the In vivo fluorescence technique. *Chesapeake Science* 16: 79-92. doi:10.2307/1350685
- Maritorena S., D.A. Siegel, and A. Peterson. 2002. Optimization of a semianalytical ocean color model for global-scale applications. *Appl. Opt.* **41**: 2705-2714.
- Mitchell, B.G., M. Kahru, and J. Sherman. 2000. Autonomous temperature-irradiance profiler resolves the spring bloom in the Sea of Japan. *Proceedings, Ocean Optics XV, Monaco, October 2000.*
- Oubelkheir, K., Claustre, H., Babin, M., and Sciandra, A. 2005. The comparative bio-optical and biogeochemical properties of contrasted trophic regimes. *Limnol. Oceanogr.* **50**: 1795-1809.
- Reynolds, R. A., D. Stramski, and B. G. Mitchell. 2001. A chlorophyll-dependent semianalytical reflectance model derived from field measurements of absorption and backscattering coefficients within the Southern Ocean. *J. Geophys. Res.* **106**: 7125–7138.
- Riley, G.A., H. Stommel, and D.F. Bumpus. 1949. Quantitative ecology of the plankton of the Western North Atlantic. *Bull. Bingham Oceanogr. Coll.* **12(3)**: 1-169.
- Sackmann, B.B. 2007. Remote assessment of 4-D phytoplankton distributions off the Washington coast. Ph.D. dissertation, University of Maine.

- Smetacek, V., and U. Passow. 1990. Spring bloom initiation and Sverdrup's critical-depth model. *Limnol. Oceanogr.* **35**: 228-234.
- Smith, R.D., M.E. Maltrud, F.O. Bryan, and M.W. Hecht. 2000. Numerical simulation of the North Atlantic Ocean at  $1/10^\circ$ . *J. Phys. Oceanogr.* **30**: 1532–1561.
- Spinrad, R.W., and J.R.V. Zaneveld. 1982. An analysis of the optical features of the near-bottom and bottom nepheloid layers in the area of the Scotian Rise. *J. Geophys. Res.* **87**: 9553-9561.
- Strutton, P.G. and F.P. Chavez. 2003. Scales of biological-physical coupling in the equatorial Pacific. *In* L. Seuront and P.G. Strutton [eds.], *Handbook of scaling methods in aquatic ecology*. CRC Press, Boca Raton, FL.
- Sverdrup, H. U. 1953. On conditions for the vernal blooming of phytoplankton. *J. Conseil Exp. Mer.* **18**: 287.
- Wang, J., G. F. Cota, and D. A. Ruble. 2005. Absorption and backscattering in the Beaufort and Chukchi Seas. *J. Geophys. Res.* **110**, C04014, doi:10.1029/2002JC001653.
- Westberry, T., M.J. Behrenfeld, D.A. Siegel, and E. Boss. 2007. Carbon-based primary productivity modeling with vertically resolved photoacclimation. *Global Biogeochem. Cycles*, submitted.

## Figure Legends

Fig. 1. Float trajectory.

Fig. 2. Measurements of temperature, salinity, backscattering at 440nm and chlorophyll at depths deeper than 970m. The two lines denote the crossing of the Gulf Stream (left) and the center of the eddy event (see text).

Fig. 3. Time series of the particulate backscattering coefficient at 440nm and chlorophyll concentration obtained from inverting satellite ocean color and from the float sensor. The float sensor data was converted to chlorophyll concentration and  $b_{bp}(440)$  by vicariously calibrating it with the same ocean color data (from which the single slope parameter was obtained, see text).

Fig. 4. Particulate backscattering coefficient at 440nm vs. chlorophyll data acquired by the float at the upper ten meter (black) and the upper 300m of the water column. In addition, four published relationships are overlaid (lines). Note that a factor of 1.25 was used to multiply relationships providing  $b_{bp}(550)$  as a function of chlorophyll to obtain  $b_{bp}(440)$  for inclusion in the figure based on assuming a  $\lambda^{-1}$  spectral functionality for  $b_{bp}$ .

Fig. 5. Lag correlation for near-surface chlorophyll, backscattering, density, salinity and temperature. Temporal averages were removed from all variables prior to computing the lag correlation.

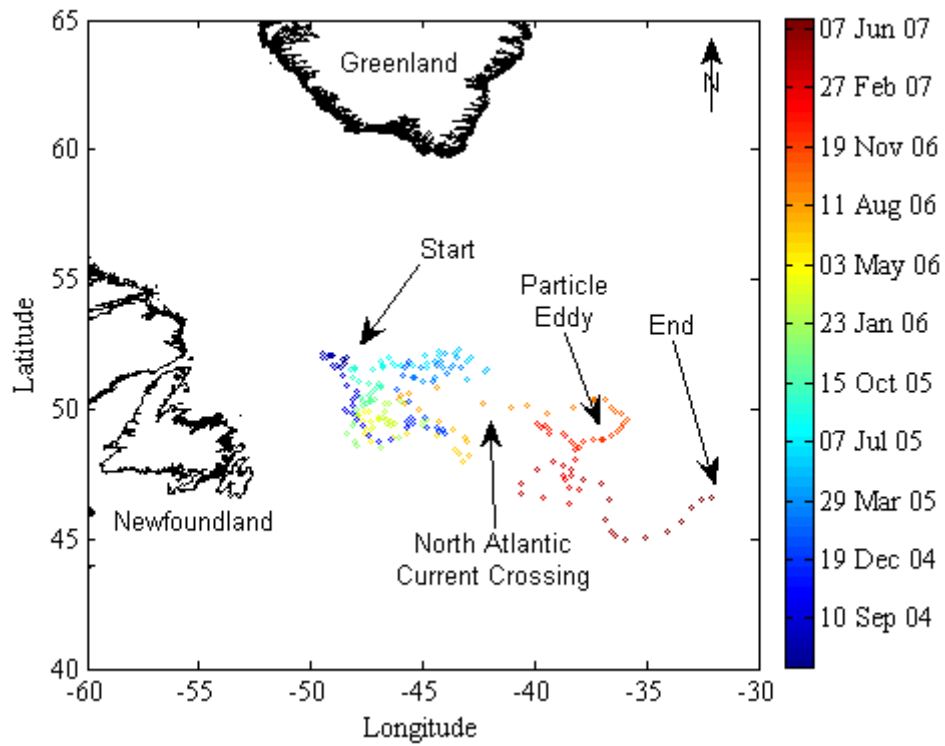
Fig. 6. Evolution of density,  $\log_{10}$  backscattering at 440nm, and  $\log_{10}$  chlorophyll and  $\log_{10}$  of the ratio of chlorophyll to backscattering as a function of time and depth throughout the life of the float in the upper 300m. The black line denotes the mixed layer depth based on the depth where the density is  $0.125\text{kg/m}^3$  higher than near the surface.

Fig. 7. Evolution of chlorophyll, density, backscattering and temperature as a function of time for five depths bins. Lines represent the median of properties values for data in the following depth bins: [0-30db], [75-130db], [185-245db], [315-480db], and [750-1050db]. Each bin contains approximately five sampling depths. The two vertical lines denote the crossing of the Gulf Stream and the center of the period when the float was sampling an eddy.

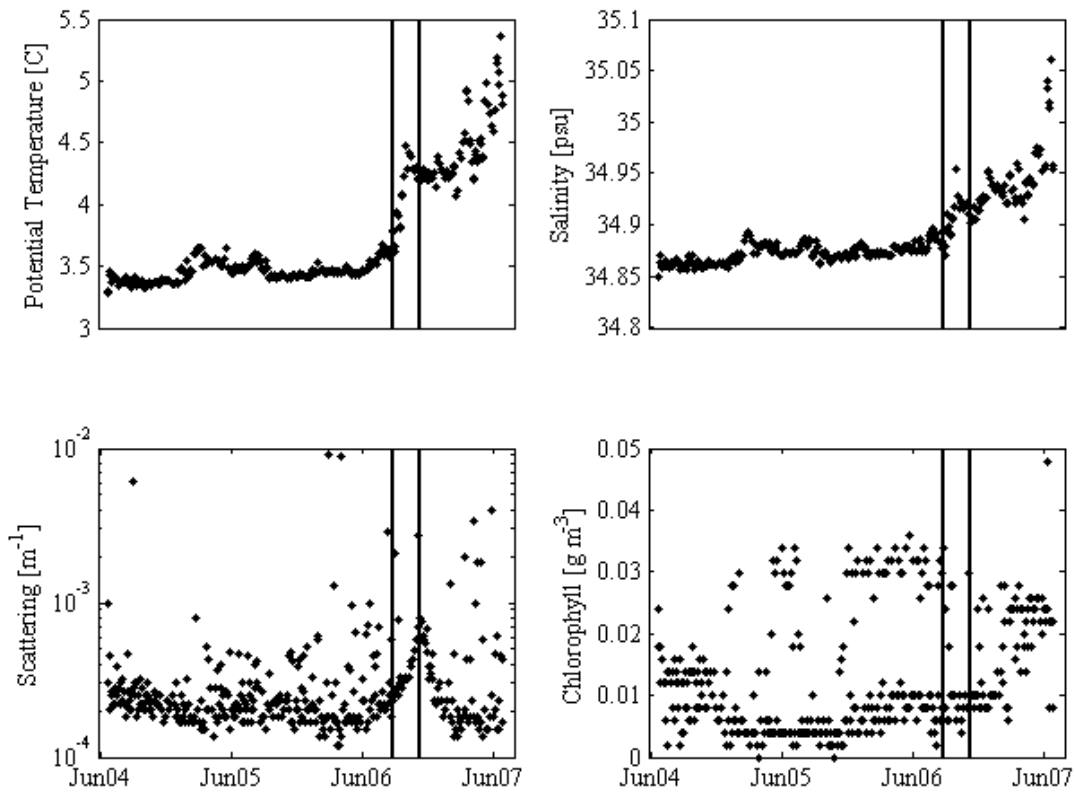
Fig. 8. Number of data points in each month (circle-float, star-satellite) and coefficient of variation of chlorophyll (based on float, line) as a function of time.

Fig. 9. Float trajectory from 1 September to 31 December 2006 overlaid on a contour of sea surface anomaly (in cm) obtained for 18 October 2006. Note the anti-cyclonic eddy centered at 50N 37W. This feature was quasi-stationary at this location for longer than two months.

Fig. 10. Integrated chlorophyll (thick line) and particulate backscattering (thin line) from the surface to 300db depth.

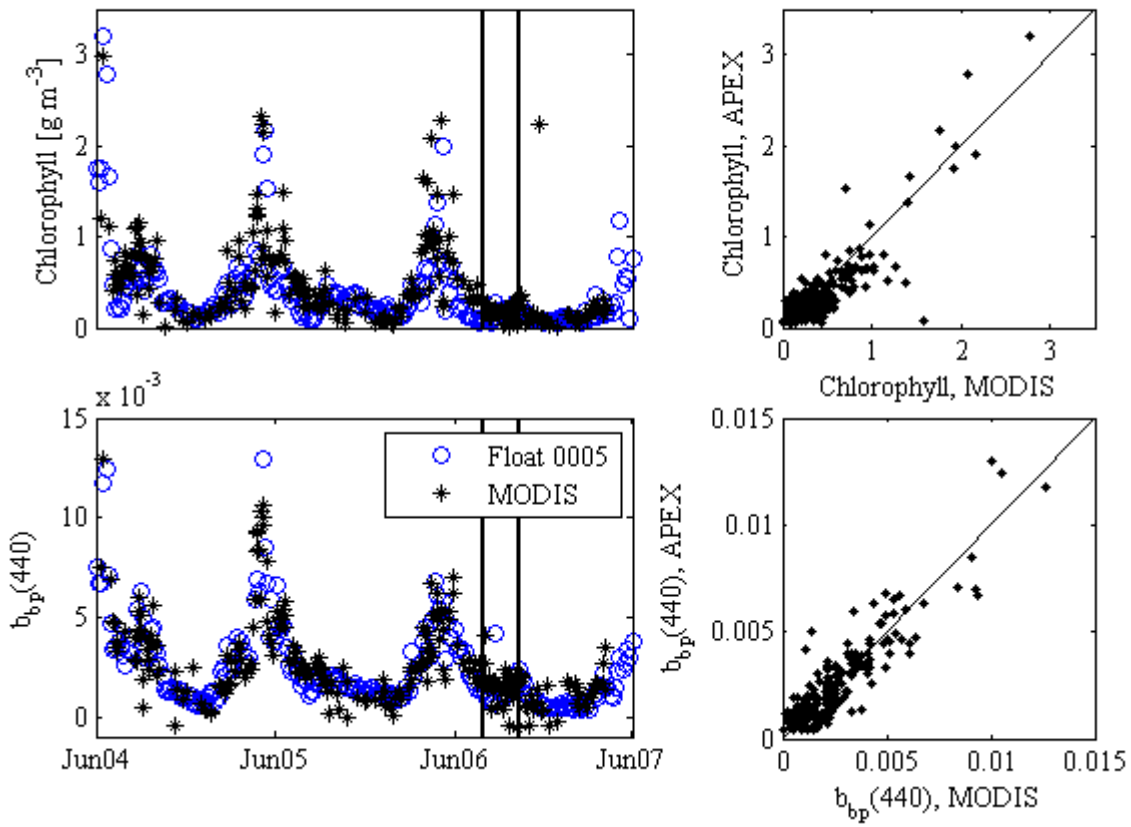


-E. Boss Fig 1-

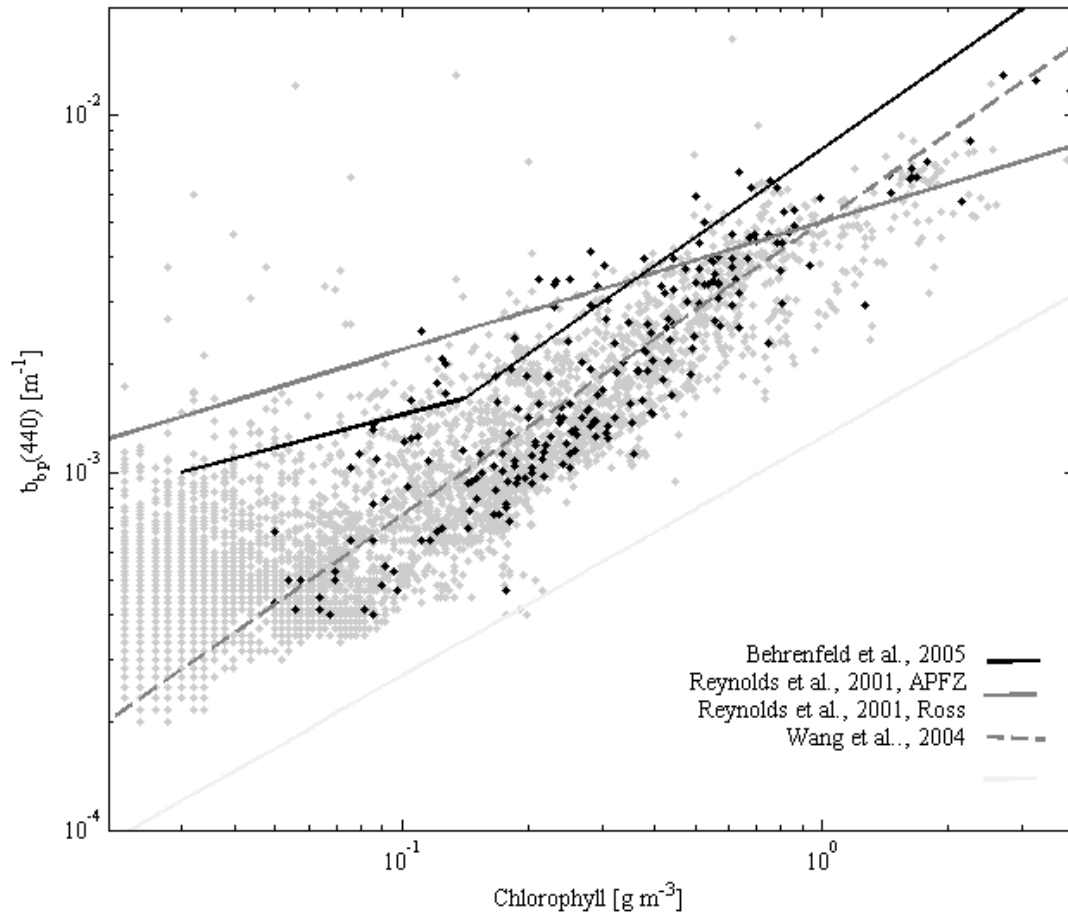


-E. Boss Fig 2-

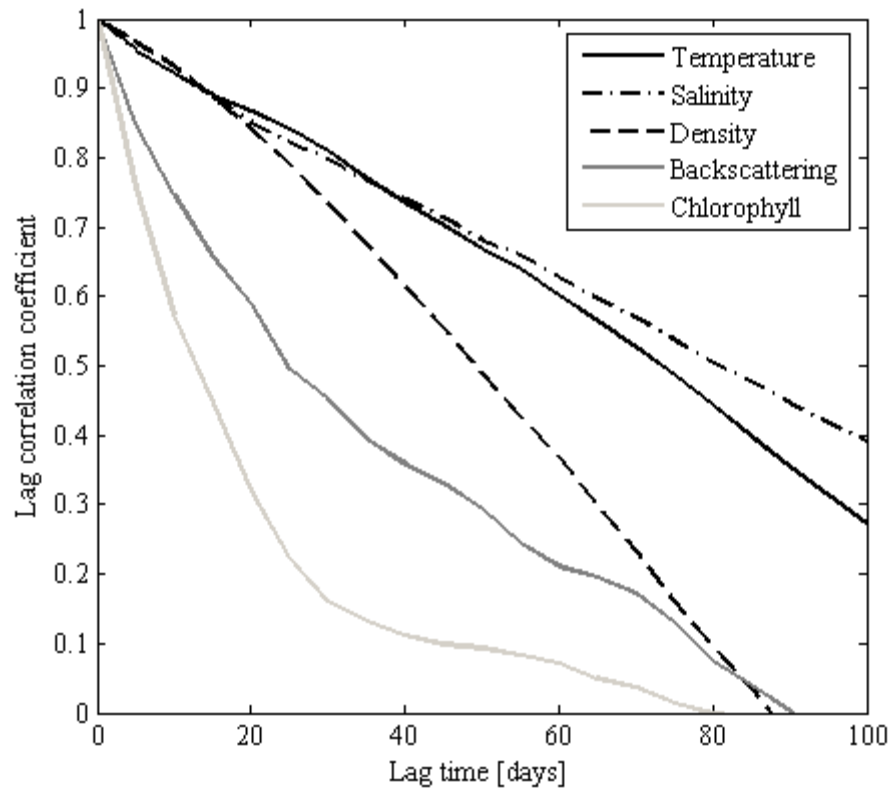


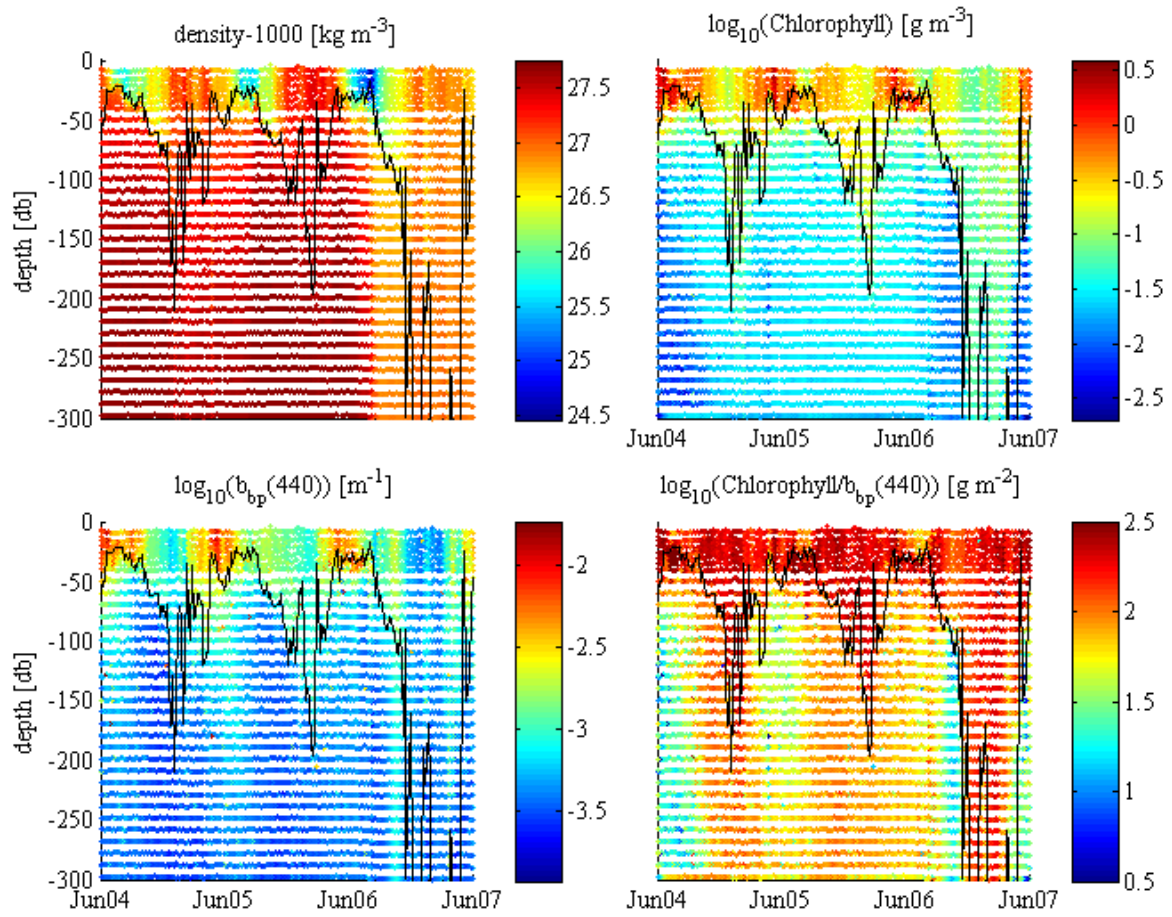


-E. Boss Fig 3-

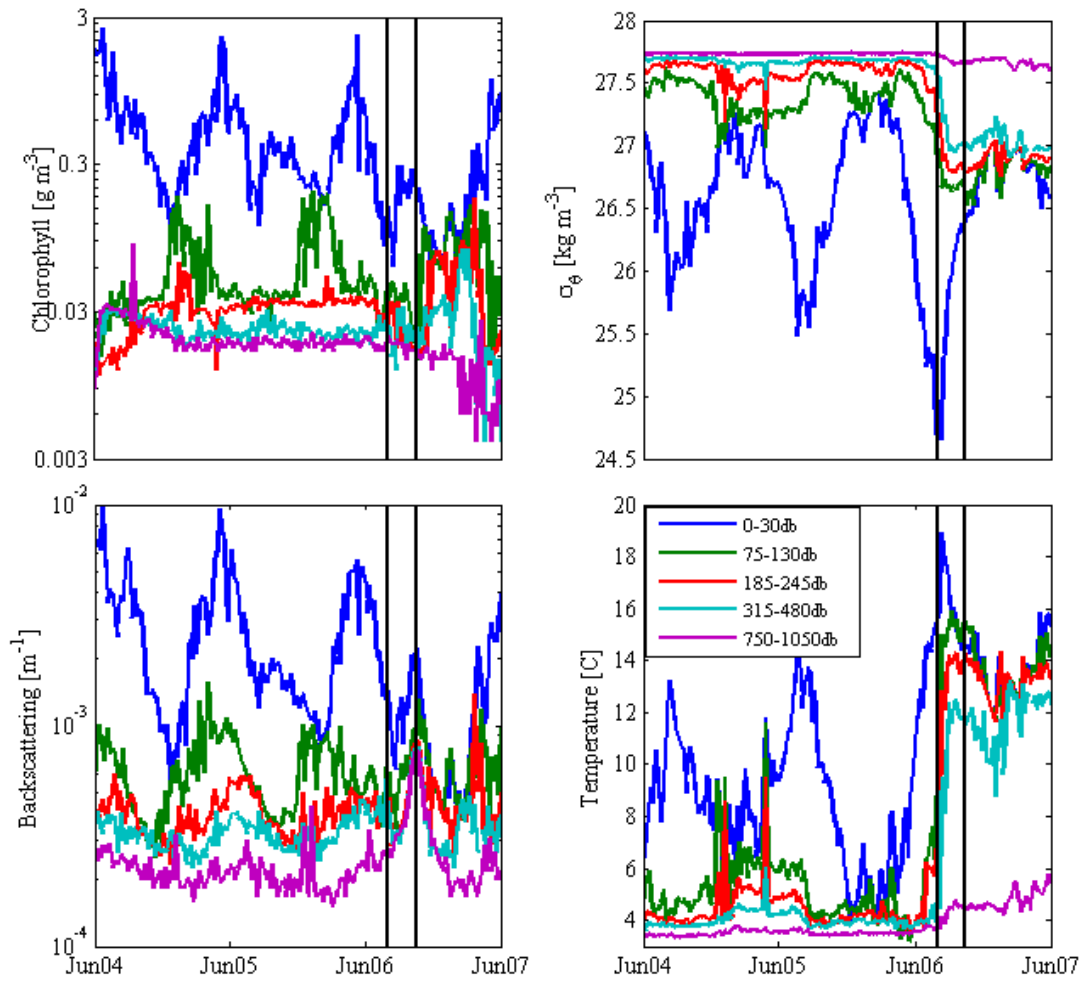


-E. Boss Fig 4-

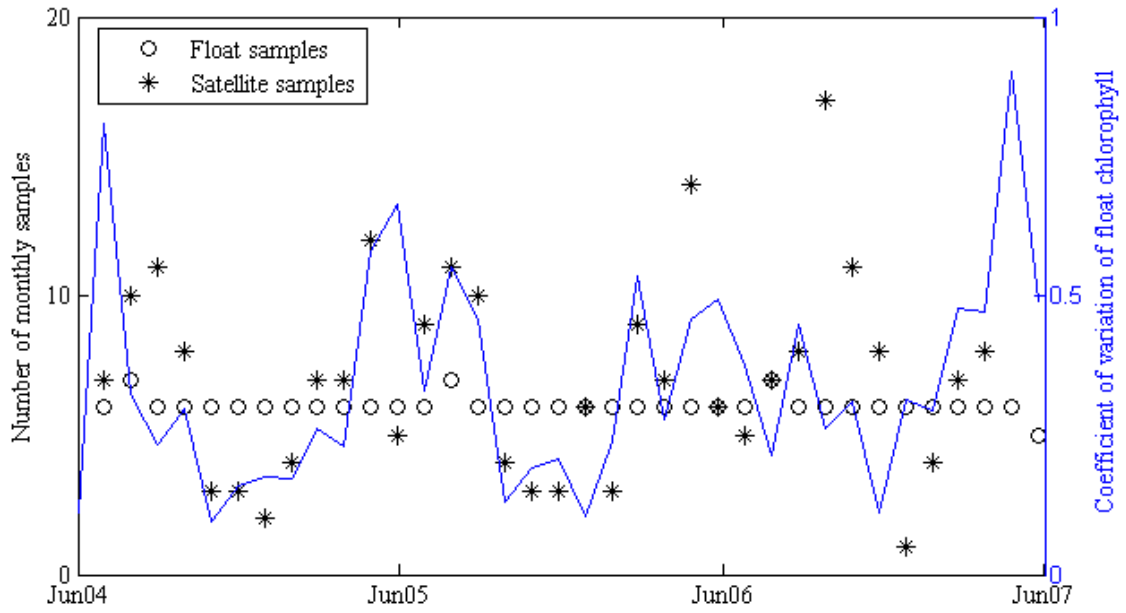




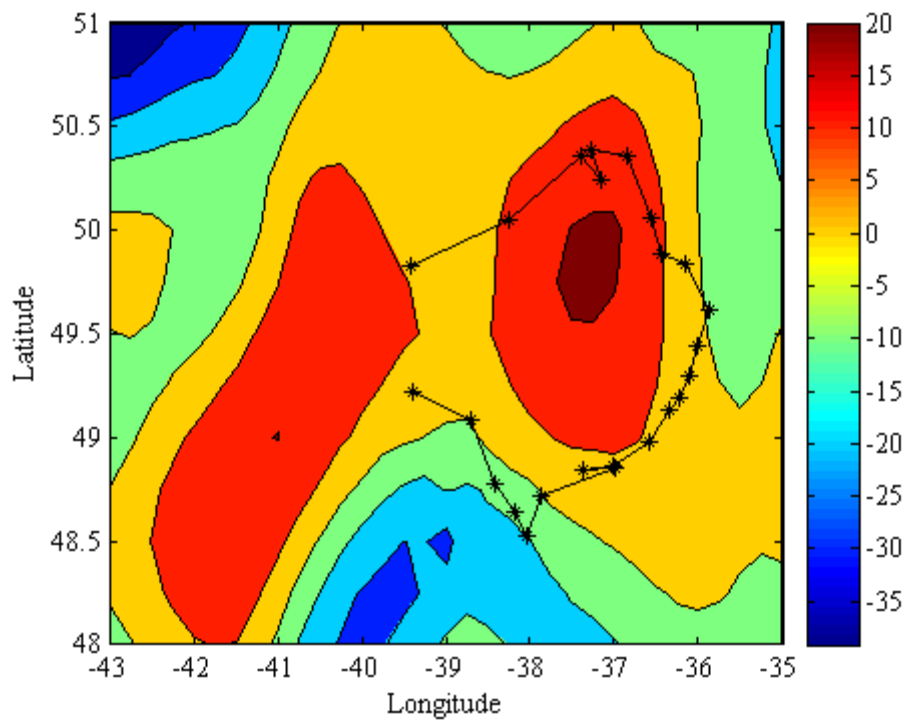
-E. Boss Fig 6-



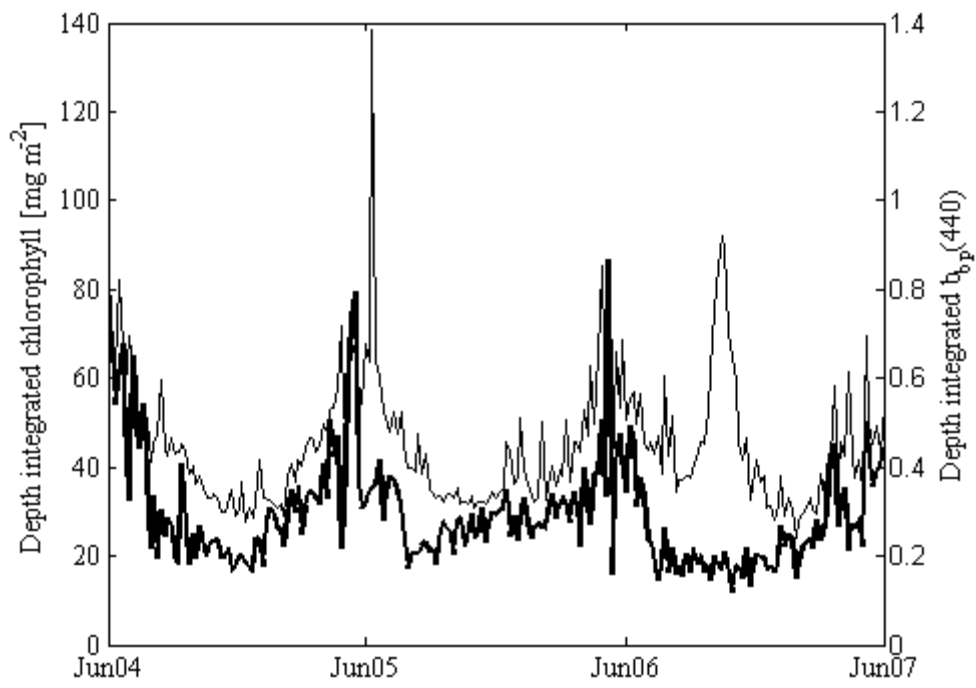
-E. Boss Fig 7-



-E. Boss Fig 8-



-E. Boss Fig 9-



-E. Boss Fig 10-